Cell Stress and Chaperones (2014) 19:241–254
DOI 10.1007/s12192-013-0450-y

ORIGINAL PAPER

Golgi fragmentation induced by heat shock or inhibition of heat shock proteins is mediated by non-muscle myosin IIA via its interaction with glycosyltransferases

Armen Petrosyan · Pi-Wan Cheng

Received: 3 May 2013 / Revised: 23 July 2013 / Accepted: 24 July 2013 / Published online: 30 August 2013

Abstract The Golgi apparatus is a highly dynamic organelle which frequently undergoes morphological changes in certain normal physiological processes or in response to stress. The mechanisms are largely not known. We have found that heat shock of Panc1 cells expressing core 2 *N*-acetylglucosaminyltransferase-M (Panc1-C2GnT-M) induces Golgi disorganization by increasing non-muscle myosin IIA (NMIIA)–C2GnT-M complexes and polyubiquitination and proteasomal degradation of C2GnT-M. These effects are prevented by inhibition or knockdown of NMIIA. Also, the speed of Golgi fragmentation induced by heat shock is found to be positively correlated with the levels of C2GnT-M in the Golgi. The results are reproduced in LNCaP cells expressing high levels of two endogenous glycosyltransferases—core 2 *N*-acetylglucosaminyltransferase-L:1 and β-galactoside:α2-3 sialyltransferase 1. Further, during recovery after heat shock, Golgi reassembly as monitored by a Golgi matrix protein giantin precedes the return of C2GnT-M to the Golgi. The results are consistent with the roles of giantin as a building block of the Golgi architecture and a docking site for transport vesicles carrying glycosyltransferases. In addition, inhibition/depletion of HSP70 or HSP90 in Panc1-C2GnT-M cells also causes an increase of NMIIA–C2GnT-M complexes and NMIIA-mediated Golgi fragmentation but results in accumulation or degradation of C2GnT-M, respectively. These results can be explained by the known functions of these two HSP: participation of HSP90 in protein folding and HSP70 in protein folding and degradation. We conclude that NMIIA is the master regulator of Golgi fragmentation induced by heat shock or inhibition/depletion of HSP70/90.

Keywords Heat shock · Heat shock protein 70 and 90 · Golgi fragmentation · Glycosyltransferase · Non-muscle myosin IIA

Abbreviations

C2GnT-M/2	Core 2β1,6 *N*-acetylglucosaminyltransferase mucus-type or isozyme 2
C2GnT-L/1	Core 2β1,6 *N*-acetylglucosaminyltransferase leukocyte-type or isozyme 1
GT	Glycosyltransferases
ER	Endoplasmic reticulum
GA	Geldanamycin
HS	Heat shock
HSP	Heat shock proteins
NMIIA	Non-muscle myosin IIA
KD	Knockdown

Introduction

The Golgi apparatus is a membrane-bound organelle located near the nucleus of most eukaryotic cells. The Golgi is the "heart" of the intracellular transportation where the proteins synthesized in the rough endoplasmic reticulum (ER) are processed and sorted before transported to other cellular organelles or secreted (Morré and Mollenhauer 2009). The Golgi contains stacks of flattened ribbon-like structure made of matrix and residential proteins (Marsh 2002). The matrix proteins, such as GM130, GRASP65, and giantin, serve as the building blocks of the Golgi architecture (Pfeffer 2001; Ward

A. Petrosyan · P.-W. Cheng
Department of Research Service, Veterans Administration Nebraska-Western Iowa Health Care System, Omaha, NE, USA

A. Petrosyan · P.-W. Cheng (✉)
Department of Biochemistry and Molecular Biology, College of Medicine, University of Nebraska Medical Center, Omaha, NE 68198-5870, USA
e-mail: pcheng@unmc.edu

P.-W. Cheng
Eppley Institute for Research in Cancer and Allied Diseases, University of Nebraska Medical Center, Omaha, NE, USA

et al. 2001; Barr and Short 2003) and the docking sites for the transport vesicles that carry various cargoes, including glycosyltransferases (GT) (Petrosyan et al. 2012b). GT are major members of the Golgi resident proteins, which participate in the synthesis of glycoconjugates. They are type II membrane proteins that contain a short amino-terminal cytoplasmic tail, a transmembrane domain, a luminal stem or stalk region, and a large carboxy-terminal catalytic domain (Burke et al. 1994; Paulson and Colley 1989). The N-terminal region of GT contains Golgi targeting and retention signals (Grabenhorst and Conradt 1999; Osman et al. 1996; Uliana et al. 2006). Recently, we found that the cytoplasmic tail of core 2 *N*-acetylglucosaminyltransferase-L/1 (C2GnT-L/1) is not only necessary but also sufficient for the Golgi targeting and retention of this enzyme (Ali et al. 2012). C2GnT-L is retained in the Golgi by binding to Golgi phosphoprotein 3 via its cytoplasmic tail.

The Golgi apparatus is a highly dynamic organelle which is held in place by association with microtubules, actin–spectrin network, and intermediate filaments (Allan et al. 2002; Kumemura et al. 2004). It constantly undergoes dynamic changes under normal physiological conditions and reversible or irreversible fragmentation under stress (White et al. 2001; Hicks and Machamer 2005). For example, apoptosis is accompanied by irreversible disorganization of the Golgi (Hicks and Machamer 2005). In most cases, Golgi fragmentation is reversible. They include mitosis (Puri et al. 2004; Morré and Mollenhauer, 2009), treatment with many pharmacological drugs, such as alcohol (Siddhanta et al. 2003), colchicine (Pavelka and Ellinger 1983), nocodazole (Rogalski et al. 1984), cytochalasin D (Rosso et al. 2004), and brefeldin A (Klausner et al. 1992). Disruption of the Golgi also can be caused by ceramide and sphingosine (Hu et al. 2005), knockdown (KD) of COPI subunit, β-COP (Petrosyan and Cheng 2013), or inhibition of Golgi-mediated glycosylation (Xu et al. 2010). It has been reported in many neurodegenerative diseases (Gonatas et al. 2006) and colonic cancers (Egea et al. 1993; Kellokumpu et al. 2002; Petrosyan and Cheng 2013) as well. Accumulation of misfolded proteins can induce ER stress, which prevents their Golgi targeting, causing Golgi disorganization (Graves et al. 2001). In addition, accumulation of mutant proteins in the ER can lead to depletion of several chaperones, including heat shock protein 70, which results in Golgi fragmentation (Numata et al. 2013).

Recently, it was reported that non-muscle myosin IIA (NMIIA) was associated with the Golgi stacks (Sahlender et al. 2005; Fath 2005). Subsequently, we found that Golgi GT and not matrix proteins are the binding partners of NMIIA (Petrosyan et al. 2012b). Under basal conditions, NMIIA is involved in Golgi remodeling by transporting Golgi GT in a COPI-independent process to the ER to be degraded by the proteasome (Durán et al. 2003; Petrosyan et al. 2012a). Under stress conditions, such as treatment with brefeldin A or KD of β-COP, the interaction of NMIIA and Golgi GT participates in Golgi fragmentation (Petrosyan and Cheng 2013). The Golgi disorganization induced by brefeldin A or KD of β-COP can be prevented by depletion or inhibition of NMIIA. Also, Golgi fragmentation found in colon cancer cells can be reversed to compact morphology by either treatment. However, depletion or inhibition of NMIIA cannot prevent the Golgi collapse induced by nocodazole, a microtubule-disruptive agent, or cytochalasin D, an actin destabilization agent, because NMIIA is not involved in these processes (Petrosyan and Cheng 2013).

It is well established that heat shock (HS) treatment or inhibition of heat shock proteins (HSP) results in Golgi disruption and fragmentation (Chen and Balch 2006; Wang et al. 1998; Welch and Suhan 1985). However, the precise mechanisms are not known. We found that the interaction of NMIIA and Golgi GT is responsible for the Golgi fragmentation induced by HS or inhibition/depletion of HSP. HS or inhibition/depletion of HSP90 causes proteasomal degradation of GT, but inhibition/depletion of HSP70 results in accumulation of GT in the ER. The differential effect of inhibition/depletion of HSP70 versus HSP90 is consistent with the known functions of these two HSPs.

Materials and methods

Materials

The reagents used in this study were obtained from the following suppliers: KNK437, EMD Chemicals (Brookfield, WI, USA); geldanamycin, Cayman Chemical (Ann Arbor, MI, USA); blebbistatin, mouse monoclonal anti-β-actin and rabbit polyclonal antibodies (Abs) against actin and heavy chain of NMIIA and NMIIB, all from Sigma (St. Louis, MO, USA). Rabbit anti-NMIIA Ab was raised against the peptide GKADGAEAKPAE located at the C-terminus of the heavy chain of NMIIA. C-Myc (mouse monoclonal and rabbit polyclonal) and γ-tubulin (mouse monoclonal) Abs were obtained from Santa Cruz Biotechnology (Santa Cruz, CA, USA). Rabbit polyclonal Abs (anti-giantin, anti-ubiquitin), mouse monoclonal anti-HSP70, anti-HSP90, and anti-β-actin Abs which were purchased from Abcam (Cambridge, MA, USA), and mouse polyclonal Abs anti-C2GnT-L and anti-ST3Gal1 from Abnova (Taipei, Taiwan). The horseradish peroxidase-conjugated secondary Abs (donkey anti-rabbit and donkey anti-mouse) were obtained from Jackson ImmunoResearch (West Grove, PA, USA).

Cell culture, heat shock, and drug treatment

Panc1-bC2GnT-M (c-Myc) cells were prepared as previously described (Choi et al. 2005). Panc1-bC2GnT-M (c-Myc) and

LNCaP cells were grown at 37 °C under 5 % CO_2 and water-saturated environment in minimum essential medium with Earle's balanced salts (MEM/EBSS) and RPMI, respectively. Both media contained 1.5 mmol/L L-glutamine (Thermo Fisher Scientific, Inc, Waltham, MA, USA), 10 % fetal bovine serum, and antibiotics (50 U/ml penicillin and 50 μg/ml streptomycin). Geldanamycin, blebbistatin and KNK437 were dissolved in dimethyl sulfoxide (DMSO) immediately before use. Cells treated with a corresponding amount of DMSO served as controls. Working concentrations of blebbistatin and KNK437 for Panc1-bC2GnT-M (c-Myc) cells were 35 and 100 μM, respectively. The dose-dependent effect of HSP90 inhibition was examined using 5 and 10 μM of geldanamycin (GA). For HS treatment, the cells were exposed to growth medium preheated to 45 °C and incubated for up to 20 min in a 45 °C water bath. After HS, the cells were allowed to recover under regular culture conditions for various durations as described in each experiment. To examine the effect of NMIIA inhibition, Panc1-bC2GnT-M (c-Myc) and LNCaP cells were treated with 35-μM blebbistatin or appropriate amount of DMSO followed by HS. In another series of experiments prior to HS, Panc1-bC2GnT-M (c-Myc) cells were treated with scramble, NMIIA, or NMIIB siRNA, and LNCaP cells were treated with scramble, NMIIA, or 150 nM C2GnT-L+150 nM ST3Gal1 siRNAs for 72-96 h. To determine the role of HSP70 inhibition in Golgi fragmentation, Panc1-bC2GnT-M (c-Myc) cells were treated with 100 μM KNK437. To assess the role of NMIIA in the Golgi fragmentation, cells were incubated with 35-μM blebbistatin for 1 h followed by 100 μM KNK437. Alternatively, cells were treated with 250 nM HSP70 siRNA for 72 h, or 200 nM NMIIA plus 250 nM HSP70 siRNAs for 96 h. To examine the role of HSP90 in maintaining the Golgi morphology, Panc1-bC2GnT-M (c-Myc) cells were treated with 5 or 10 μM of GA for 2 h or 35 μM blebbistatin for 1 h followed by 10 μM of GA. The specific contribution of HSP90β1 isoform to the maintenance of the Golgi morphology was examined by treating the cells with 200 nM of Hsp90β1 siRNA or 200 nM NMIIA plus 200 nM Hsp90β1 siRNAs.

Co-immunoprecipitation and transfection

For identification of proteins in the complexes pulled down by co-immunoprecipitation (Co-IP), confluent Panc1-bC2GnT-M (c-Myc) and LNCaP cells grown in a T75 flask were washed three times with 6 ml phosphate-buffered solution (PBS) each, harvested by trypsinization, and neutralized with soybean trypsin inhibitor at a 2× weight of trypsin. After washing three times with PBS, the cells were lysed with 1.5 ml of a non-denaturing lysis buffer, which contained 50 mM Tris (pH 7.4), 150 mM NaCl, 5 mM EDTA, 0.5 % NP-40 (*w*/*w*), and 1 % (*v*/*v*) of mammalian protease inhibitor cocktail (Sigma). One milliliter of cell lysate was pre-cleared by treatment with 50 μl of irrelevant antibody (1 mg/ml) of same species and isotype to be employed for IP at 4 °C for 1 h. The process was followed by incubation with 100 μl of 50 % slurry of protein G plus agarose (EMD) at 4 °C for 1 h with gentle rocking. After centrifugation, an aliquot of the supernatant was incubated with anti-c-Myc (for C2GnT-M) or anti-C2GnT-L and anti-ST3Gal1 Ab (1.5 μg Abs to 400 μg protein in 1-ml cell lysate) overnight at 4 °C with gentle rocking. Then, 50 μl of protein G agarose slurry was added and incubated at 4 °C for 1 h with gentle rocking to capture the immunocomplexes. The pellet was resuspended in lysis buffer and washed with PBS three times. The last pellet was resuspended in SDS sample buffer. MYH9 (NMIIA, myosin, heavy polypeptide 9, non-muscle), HSPA8 (heat shock 70 kDa protein 8), HSP90β1 (heat shock protein 90, beta), and scrambled On-Targetplus Smartpool siRNA were purchased from Dharmacon (Chicago, IL, USA). The pool of three siRNAs targeting ST3Gal1 and GCNT1 (C2GnT-L) was obtained from Santa Cruz Biotechnology. Panc1-bC2GnT-M (c-Myc) and LNCaP cells were transfected with 150–250 nM siRNAs using Lipofectamine RNAi MAX reagent and MEM/EBSS without antibiotics according to the manufacturer's recommendation. After culture for 72–96 h, cells were analyzed by western blotting as described below.

Proteins were separated on sodium dodecyl sulfate polyacrylamide gel electrophoresis (SDS-PAGE) on mini-gels with various percentages of gel specified for each experiment (Bio-Rad, Hercules, CA). western blots were developed using HRP-coupled antibodies and Thermo Scientific SuperSignal West Pico Chemiluminescent Substrate reagents and then exposed to BioExpress Blue Basic Autorad chemiluminescence film (Kaysville, UT, USA). The bands on the autoradiography films were digitized by scanning with ScanJet 6200C (Hewlett Packard) driven by Adobe Photoshop.

Confocal immunofluorescence microscopy

Panc1-bC2GnT-M (c-Myc) and LNCaP cells were grown overnight on cover slips placed in a 6-well plate. After washing twice with PBS, the cells were immediately fixed in 4 % paraformaldehyde/PBS for 30 min at RT. Then, the cells were incubated with primary Abs (1:100) at 37 °C for 1 h. After washing with phosphate-buffered saline/Tween (PBST) three times, the cells were stained with fluorochrome-conjugated DyLight 488 donkey anti-mouse Ab (green) and DyLight 594 donkey anti-rabbit Ab (red) (1:200) (Jackson Immuno Research). After the final wash with PBST, the cells were mounted in ProLong Gold antifade reagent with or without DAPI (Invitrogen). The stained cells were viewed under a Zeiss 510 Meta Confocal Laser Scanning Microscope performed at the Confocal Microscopy Core Facility of the University of Nebraska Medical Center. Fluorescence was detected using an emission filter of 417 to 477 nm band pass

for DAPI, 505 to 550 nm band pass for green, and 575 to 615 nm band pass for red. Images were analyzed using Zeiss 510 software. For some figures, image analysis was performed using Adobe Photoshop and the ImageJ. The average fluorescence intensity was measured as a mean±SEM of integrated fluorescence intensity (in arbitrary units, a.u.) measured for every cell individually. The percentage of the cells exhibiting Golgi fragmentation was counted in at least 90 cells from three independent experiments. Cells with giantin staining distributed throughout the cell with only a small amount of perinuclear staining were qualified as cells with fragmented Golgi. The number of Golgi fragments per cell was defined by giantin immunostain covering more than 500 nm in size.

Isolation of Golgi membrane and cytoplasm fractions by sucrose gradient flotation

The preparation of Golgi membranes was performed with the methods described previously (Petrosyan and Cheng 2013). Panc1-bC2GnT-M (c-Myc) cells from ten to twelve 75-cm^2 cell culture flasks were harvested by PBS containing 0.5× protease inhibitors (1.2 ml per flask). Then, after centrifugation for 5 min at 1,000 rpm and 4 °C, the pellet was resuspended in 3 ml of homogenization buffer (0.25 M sucrose, 3 mM imidazole, 1 mM Tris–HCl; pH 7.4, 1 mM EDTA). The cells were homogenized by drawing ~30 times through 25-gauge needle until the ratio between unbroken cells and free nuclei becomes 20:80 %. The postnuclear supernatant was obtained by centrifugation at 2,500 rpm in a microfuge and 4 °C for 3 min, and then the supernatant was adjusted to 1.4 M sucrose by the addition of ice-cold 2.3 M sucrose containing 10 mM Tris–HCl (pH 7.4). Next, 1.2 ml of 2.3 M sucrose at the bottom of tube was loaded by 1.2 ml of the supernatant followed by sequential overlay by 1.2 ml of 1.2 M and 0.5 ml of 0.8 M sucrose (10 mM Tris–HCl, pH 7.4). The gradients were centrifuged for 3 h at 30,000 rpm (4 °C) in SW40 rotor in an ultracentrifuge (Beckman Coulter). The turbid band at the 0.8 M/1.2 M sucrose interface containing Golgi membranes was harvested in ~500 μl by syringe puncture. The fraction at concentration of ~1.0 to 1.4 mg protein/ml was used for the experiments mentioned in "Results" section.

Isolation of HSP90 in Panc1-bC2GnT-M (c-Myc) cell lysates with biotinylated N-terminal peptides of hC2GnT-M

N-terminal biotinylated 7 aa peptide (MVQWKRL) representing the cytoplasmic tail (CT) of hC2GnT-M was obtained from the AAPPTec LLC (Louisville, KY, USA). Control biotin-GHGTGSTGSGSMLRTLLRRRL peptide was purchased from LifeTein LLC (South Plainfield, NJ, USA). To isolate HSP90, 20 μl of C2GnT-M CT peptide in 25 % acetic acid (0.1 mg/ml) was mixed with 20–40 μl of cell lysate (1.5–3.5 mg/ml of protein). After incubation at 37 °C for 1 h, 100 μl of Dynabeads M-280 Streptavidin (Dynal, Norway) was added. Following gentle rotation for additional 30 min, the beads containing immobilized complexes were trapped with a magnet. The captured proteins were separated on 8 % SDS-PAGE followed by western blotting with anti-NMIIA Abs. Control peptide was used by same procedure. Another sample of cell lysate incubated with appropriate amount of 25 % acetic acid followed by treatment with Dynabeads served as a control.

Proteomics analysis of electrophoretically separated proteins

Following separation of the proteins on SDS-PAGE, Coomassie blue-stained bands were excised and subjected to proteomics analysis which was carried out by the Mass Spectrometry and Proteomics Core Facility of the University of Nebraska Medical Center.

Miscellaneous

Protein concentrations were determined with the Coomassie Plus Protein assay (Pierce Chemical Co., Rockford, IL, USA) using BSA as the standard. Data are expressed as mean±SEM. Analysis was performed using two-sided *t* test. A value of $p<0.05$ was considered statistically significant.

Results

Heat shock-induced Golgi fragmentation is mediated by NMIIA via its interaction with glycosyltransferases

To examine the role of GT in HS-induced Golgi fragmentation, we monitored the Golgi morphology in two different populations of Panc1-bC2GnT-M (c-Myc) cells, one expressing low (L) (up to 25,000 a.u. of integrated fluorescence) and one expressing high (H) (over 25,000 a.u.) levels of C2GnT-M. As shown in Fig. 1a, b for both populations of the cells, the number of cells with fragmented Golgi was gradually increased as the HS treatment time was extended from 5 to 20 min. Further, at each time point of HS treatment, the Golgi with higher levels of C2GnT-M was more susceptible to HS-induced fragmentation as compared to the Golgi with lower levels of C2GnT-M. The calculated Spearman's rank correlation coefficient between number of Golgi fragments and C2GnT-M fluorescence intensity at every time point was statistically significant. It was 0.72 ($p<0.01$), 0.67 ($p<0.01$), 0.69 ($p<0.01$), and 0.52 ($p<0.05$) at 5, 10, 15, and 20 min of HS, respectively. The data indicate that the speed of Golgi disorganization positively correlated with intra-Golgi levels of C2GnT-M. We found that at the end of 20-min HS treatment, more NMIIA was pulled down with anti-c-Myc Ab (Fig. 1c), indicating that more NMIIA–

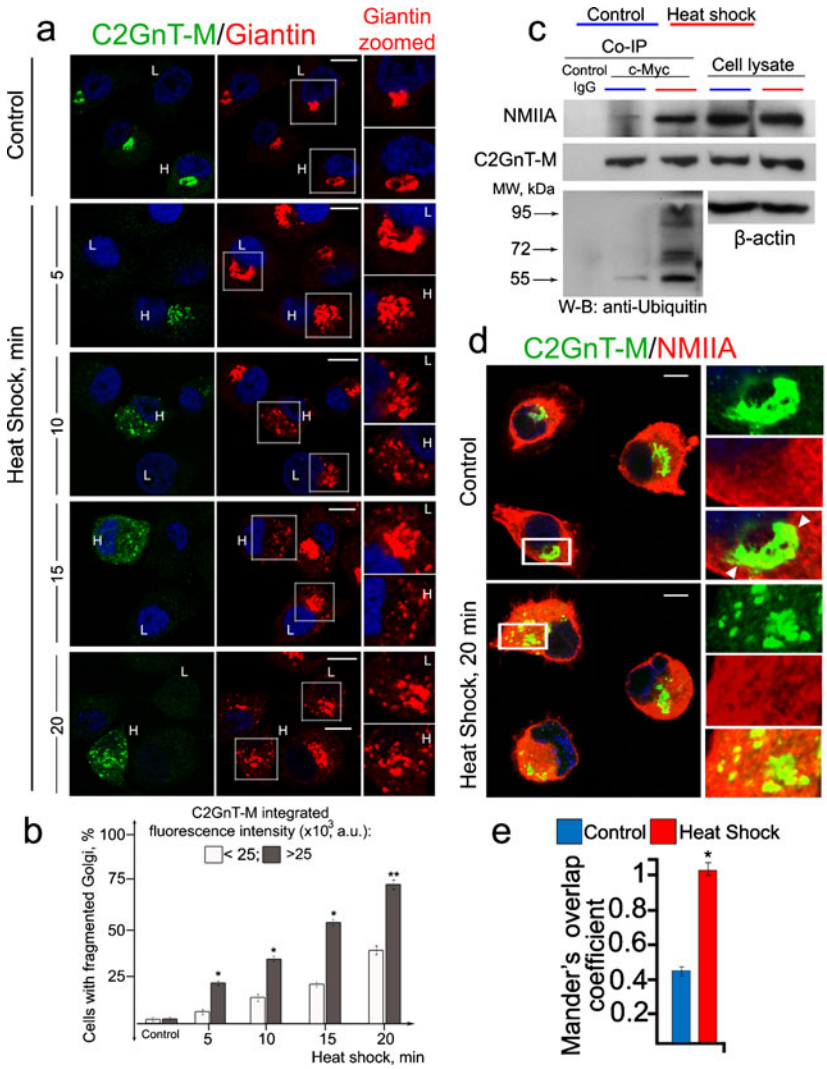

Fig 1 Morphological changes of the Golgi induced by heat shock treatment of Panc1-bC2GnT-M (c-Myc) cells. **a** Confocal immunofluorescence images of bC2GnT-M and giantin in cells heat shocked at 45 °C for up to 20 min. The breakdown of the Golgi was analyzed in 90 cells at each of 5-, 10-, 15-, and 20-min time points of HS. The giantin staining of representative cells with high (*H*) and low (*L*) expression of bC2GnT-M are presented on the *right hand side* (zoomed giantin). The cells with higher expression of C2GnT-M demonstrate greater sensitivity to HS treatment than cells with lower expression of C2GnT-M. **b** Percentage of the cells with fragmented Golgi at different time points of HS treatment in cells with low (up to 25,000 a.u.) or high (over 25,000 a.u.) C2GnT-M integrated fluorescence. *Single asterisk* indicates $p<0.01$ and *double asterisk*, $p<0.05$. **c** NMIIA, c-Myc, and ubiquitin western blots of complexes pulled down with anti-c-Myc Ab from the lysates of cells immediately after HS. Equal amounts of proteins were used for c-Myc Co-IP. **d** Confocal immunofluorescence images of C2GnT-M and NMIIA in cells immediately after HS. Partial colocalization in control cells at the boundary of the Golgi (*white arrowheads* on higher magnifications (*boxes*) on the right) was increased in abundance in heat-shocked cells. **e** Quantification of Mander's overlap coefficient of C2GnT-M and NMIIA colocalization of cells presented in **d**. Data were obtained from 90 cells in three independent experiments. *Asterisk* indicates $p<0.01$ compared to control

C2GnT-M complexes were formed. Further, more ubiquitinated C2GnT-M was detected, suggesting an increased degradation of this enzyme by proteasome (Fig. 1c). Double immunofluorescence staining of C2GnT-M and NMIIA showed a significant increase of their colocalization after only 20 min of HS (Fig. 1d) which was confirmed by increased Mander's overlap coefficients (Fig. 1e).

To determine whether NMIIA was involved in Golgi fragmentation under HS stress, we treated Panc1-bC2GnT-M (c-Myc) cells with NMIIA inhibitor, blebbistatin (35 μM) (Straight et al. 2003) at 37 °C for 1 h and then 45 °C for 10 min. We found that blebbistatin treatment suppressed the HS-induced disassembly of the Golgi (Fig. 2a). In addition, NMIIA was and NMIIB was not involved in HS-induced Golgi fragmentation because treatment with NMIIA but not NMIIB siRNA prevented the HS-induced disorganization of the Golgi (Fig. 2a, b).

To gain insight into the mechanism of Golgi fragmentation induced by HS, especially the nature of the involvement of NMIIA and C2GnT-M, we heat shocked Panc1-bC2GnT-M

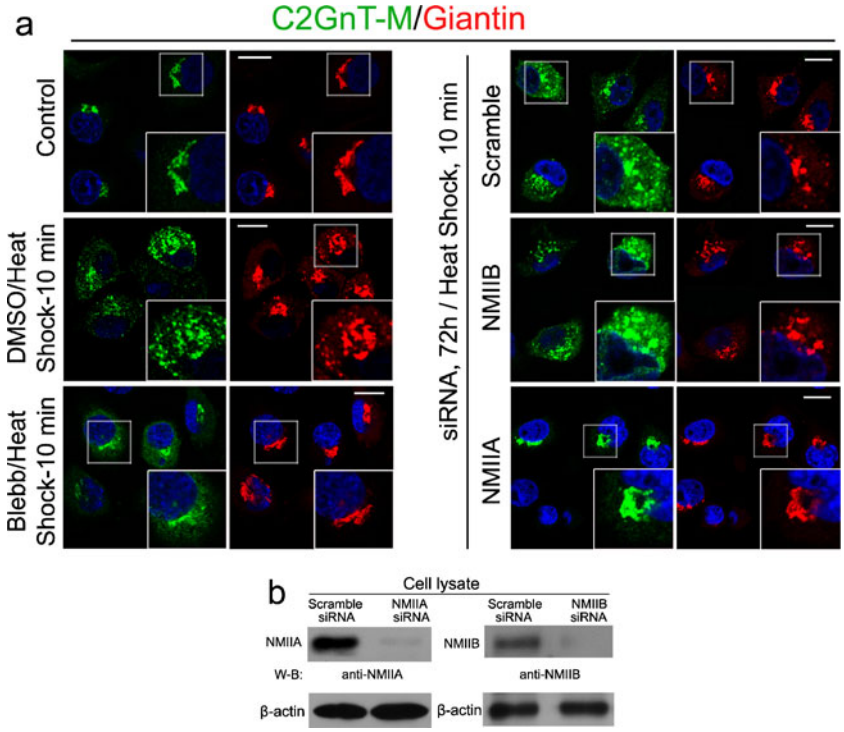

Fig. 2 NMIIA inhibition or knockdown prevents heat shock-induced Golgi fragmentation. **a** Cells were pretreated with scramble, NMIIA, or NMIIB siRNA for 72 h or 35 μM blebbistatin (Blebb) and appropriate amount of DMSO for 1 h and then underwent HS treatment for 10 min. NMIIA siRNA (but not NMIIB siRNA) or blebbistatin treatment prevented Golgi disorganization. **b** NMIIA and NMIIB western blots of the lysates of cells treated with NMIIA or NMIIB siRNA, respectively. representative pictures of at least three independent experiments are shown. All confocal images were acquired with same imaging parameters; *bars*, 10 μm

(c-Myc) cells and then monitored the levels and interactions of NMIIA and C2GnT-M, intracellular distribution of C2GnT-M, and the expression of HSP70 as a function of times post heat shock. As shown in Fig. 3a, it took about 24 h for the Golgi morphology of heat-shocked cells to fully recover, but 36 h for C2GnT-M to fully return to the Golgi. Western blot analysis of NMIIA, C2GnT-M, and HSP70 at different time points post HS showed (a) increased NMIIA at 12 and 18 h, (b) decreased C2GnT-M at 12 h, which was returned to basal level after 18 h but elevated after 24 h, and (c) elevated HSP70 at every time point between 12 and 36 h (Fig. 3b). It should be mentioned that HSP70 content was not altered for up to 8 h post HS treatment (data not shown). Further, more NMIIA was pulled down with anti-c-Myc Ab at 12 h post HS, which was returned to basal level after 18 h post HS (Fig. 3c).

To show that the phenomenon described above was not an artifact of an ectopically expressed Golgi GT (bC2GnT-M) in Panc1-bC2GnT-M (c-Myc) cells, we repeated the experiment in LNCaP cells which express high levels of two endogenous GT, C2GnT-L, and β-galactoside:α-2,3 sialyltransferase 1 (ST3Gal1) (Gao et al. 2012). We treated LNCaP cells with scramble, NMIIA, or C2GnT-L plus ST3Gal1-specific siRNAs for 72 h and then at 45 °C for 20 min. Immunofluorescence analysis of these HS-treated cells showed fragmented Golgi in cells treated with scramble siRNA but not in cells treated with either NMIIA or C2GnT-L plus ST3Gal1 siRNAs (Fig. 4a, c). Cells lacking C2GnT-L+ST3Gal1 or NMIIA retained substantially more normal Golgi morphology (85 and 92 % respectively) than the scramble siRNA or DMSO-treated control cells (35 %) (Fig. 4b). Blebbistatin treatment also prevented the HS-induced Golgi fragmentation, which yielded 93 % of the cells with normal Golgi morphology as compared to only 37 % in DMSO-treated cells (Fig. 4a, b). HS treatment also increased the amounts of NMIIA pulled down with anti-C2GnT-L or anti-ST3Gal1 Ab (Fig. 4d). These data indicate that endogenously expressed Golgi residential enzymes, such as C2GnT-L and ST3Gal1, are directly involved in NMIIA-mediated Golgi fragmentation induced by HS.

NMIIA and C2GnT-M are active participants in the Golgi disorganization induced by inhibition or knockdown of HSP70

We recently reported (Petrosyan et al. 2012a) that several isoforms of HSP70, especially heat shock 70 kDa protein 8 (HSP70-8), pulled down by anti-c-Myc Ab are required for the Golgi targeting of C2GnT-M in Panc1-bC2GnT-M (c-Myc) cells. Inhibition of HSP70 by treatment with 50 μM KNK437, a HSP70 inhibitor (Yokota et al. 2000), for 1 h or KD of 75 % of HSP70-8 by treatment with 150 nM HSP70-8 siRNA shifted the distribution of C2GnT-M from Golgi to ER but retained the Golgi architecture (Petrosyan et al. 2012a). In the current study, we found that treatment of cells with higher concentration of KNK437 (100 μM) for 1 h or HSP70-8 siRNA (250 nM) for 72 h, which resulted in 95 % KD of HSP70-8 (Fig. 5b), caused fragmentation of the Golgi but caused retention of the bulk of C2GnT-M in the cytosol (Fig. 5a, c). The Golgi breakdown induced by KNK437 was

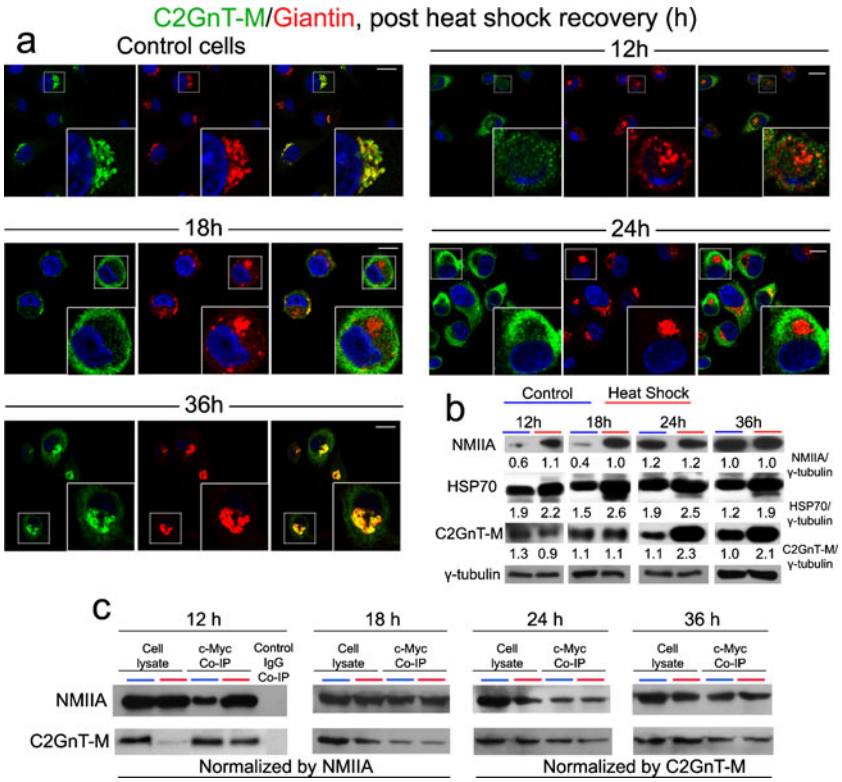

Fig. 3 NMIIA is involved in cytoplasmic mobilization of bC2GnT-M in Panc1-bC2GnT-M (c-Myc) cells during post-heat shock recovery. **a** Cells were heat-shocked at 45 °C for 20 min and allowed to recover under normal growing conditions for up to 36 h. At 12 h post HS, C2GnT-M together with giantin moved out of the fragmented Golgi. At 18 h, the Golgi (giantin) was partially recovered; however, C2GnT-M was retained in the cytoplasm. At 24 h, Golgi morphology was restored and C2GnT-M was still in the cytoplasm. After 36 h of recovery, C2GnT-M returned to the Golgi. **b** NMIIA, HSP70, and bC2GnT-M (c-Myc) western blots of the lysates obtained from cells treated by HS and allowed to recover under normal growing condition for 12, 18, 24, and 36 h. Increased NMIIA was detected at 12 and 18 h; level of HSP70 was elevated throughout the entire recovery phase; decrease of C2GnT-M was found at 12 h; no change was found at 18 h; and increased C2GnT-M was detected at 24 and 36 h. Gamma-tubulin was used as a loading control. NMIIA, HSP70, C2GnT-M, and γ-tubulin bands were analyzed by densitometry and the data were presented after normalization with γ-tubulin value. **c** NMIIA and c-Myc western blot of complexes pulled down with anti-c-Myc Ab from the lysates of cells recovered after HS for 12, 18, 24, and 36 h. At 12 h, Golgi fragmentation occurred and NMIIA–C2GnT-M complexes were elevated. Cell lysate treated with nonspecific IgG served as the negative control. Lysates containing equal amounts of NMIIA (12 and 18 h) or C2GnT-M (24 and 36 h) were used for Co-IP. Representative pictures of at least three independent experiments are shown. All confocal images were acquired with same imaging parameters; *bars*, 10 μm

inhibited by pretreatment with a NMIIA inhibitor blebbistatin (35 μM, 1 h) (Fig. 5a, c). In addition, Golgi disorganization caused by treatment with HSP70-8 siRNA was also prevented by treatment with NMIIA siRNA (Fig. 5a–c). Quantification of the Golgi morphology showed that KNK437 or HSP70-8 siRNA treatment induced disorganization of Golgi in about 80 and 66 % of the cells, respectively (Fig. 5c). Pretreatment with blebbistatin or treatment with NMIIA siRNA substantially increased the number of cells with unaffected Golgi to 79 and 85 %, respectively. Interestingly, we did not detect ubiquitinated C2GnT-M or its degradation under inhibition or KD of HSP70 (Fig. 5e). On the contrary, more C2GnT-M as measured by fluorescence intensity (Fig. 5a) or protein by western blotting was accumulated under KNK437 or HSP70-8 siRNA treatment (Fig. 5d). Treatment with either KNK437 or HSP70-8 siRNA also increased the amounts of NMIIA pulled down with anti-c-Myc Ab (Fig. 5f). The results indicate that HSP70 is required for maintaining the Golgi compact structure. Further, inhibition of HSP70 with high dosage (100 μM) of KNK437 or KD of HSP70 with high dosage (250 nM) of siRNA results in NMIIA-mediated Golgi fragmentation by increasing the formation of NMIIA–C2GnT-M complexes.

Inhibition or knockdown of HSP90 induces NMIIA and C2GnT-M-dependent fragmentation of the Golgi

We have identified by proteomics analysis many proteins (Petrosyan et al. 2012a) including HSP90β isoform a in the immunoprecipitate of anti-c-Myc Ab from the lysates of Panc1-bC2GnT-M (c-Myc) cells. The result was confirmed by another proteomics analysis following Co-IP (data not shown). We hypothesized that C2GnT-M needs the assistance of HSP90 for folding (Gonatas et al. 2006; Grad and Picard

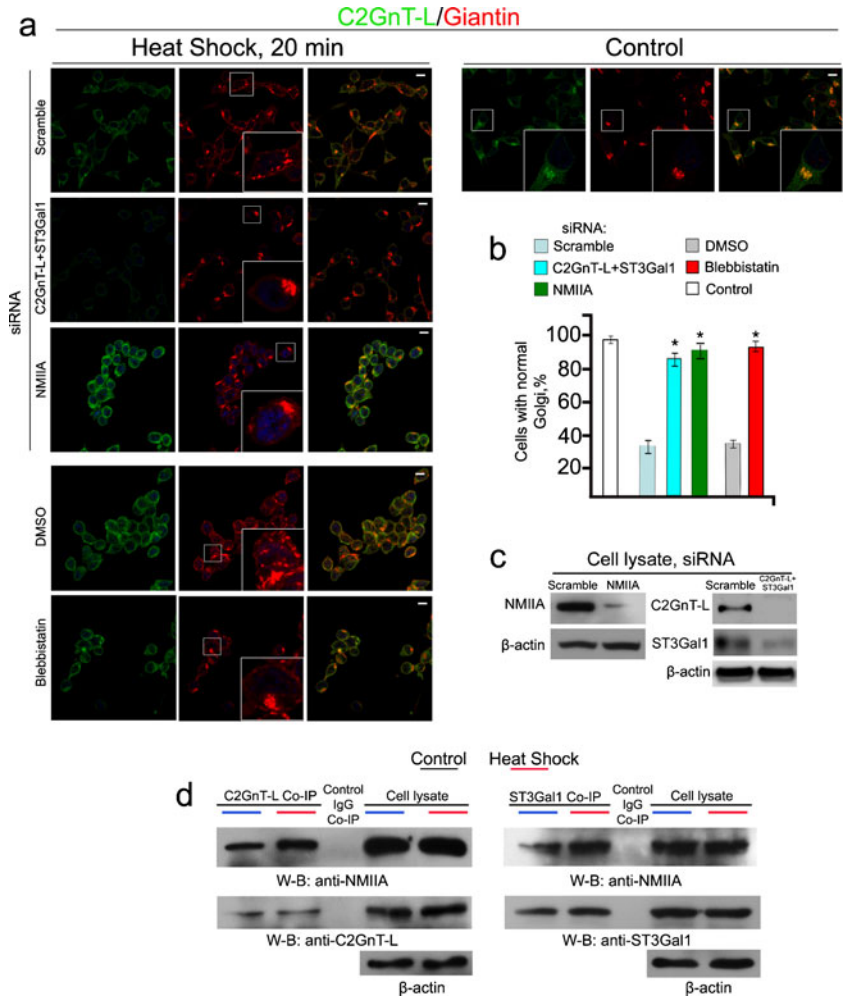

Fig. 4 Depletion of C2GnT-L and ST3Gal1 in LNCaP cells delays HS-induced Golgi disorganization. **a** Confocal immunofluorescence images of C2GnT-L and giantin in cells treated with scramble, NMIIA, or C2GnT-L+ST3Gal1 siRNAs for 72 h or 35 μM blebbistatin for 1 h and appropriate amount of DMSO followed by HS at 45 °C for 20 min. *White boxes* in the images indicate Golgi (giantin) areas enlarged in the *inset*. **b** Percentage of the cells with fragmented Golgi in cells described in **a**: KD of both C2GnT-L and ST3Gal1 delayed Golgi disorganization similar to NMIIA KD or inhibition. The data are expressed as mean±SEM; *Asterisk*, $p<0.001$. **c** NMIIA, C2GnT-L, and ST3Gal1 western blot of the lysates of cells treated with scramble, *NMIIA* (*MYH9*) or *ST3GAL1*+-*GCNT1* (*C2GnT-L*) siRNAs; beta-actin was used as a loading control. **d** NMIIA and C2GnT-L/ST3Gal1 western blots of complexes pulled down with anti-C2GnT-L or ST3Gal1 Ab from the lysates of cells immediately after HS. Cell lysates containing same amounts of proteins were used for Co-IP. The results shown are representative of three independent experiments. All confocal images were acquired with same imaging parameters; *bars*, 10 μm

2007). In this study, we found by confocal immunofluorescence microscopy that HSP90 was distributed throughout the cytoplasm including the Golgi area where it colocalized with C2GnT-M (Fig. 6a). To validate this observation, we isolated the Golgi membranes from Panc1-bC2GnT-M (c-Myc) cells. We were able to pull-down HSP90 from the Golgi fraction with c-Myc Ab, suggesting that C2GnT-M and HSP90 are associated at the Golgi membrane (Fig. 6b). Further, the N-terminally biotinylated peptide of C2GnT-M, which contained the cytoplasmic tail (1–7 aa, MVQWKRL), also pulled down HSP90 from the cell lysate (Fig. 6c). The 90-kDa Coomassie blue-stained band obtained from SDS-PAGE analysis of the proteins which was pulled down with the cytoplasmic tail of hC2GnT-M was analyzed by proteomics analysis, and many tryptic peptide sequences were matched to HSP90β isoform a (data not shown). The result suggests that the cytoplasmic tail of this enzyme forms complexes with HSP90.

Next, to determine the involvement of HSP90 in the folding of C2GnT-M, we monitored the effect of HSP90 inhibitor GA (Stebbins et al. 1997) on the intracellular distribution of C2GnT-M. We found that GA exhibited a dose-dependent effect on the ER-to-Golgi anterograde trafficking of C2GnT-M and Golgi structure. Treatment of cells with 5 μM of GA for 2 h resulted in the retention of C2GnT-M in the ER without

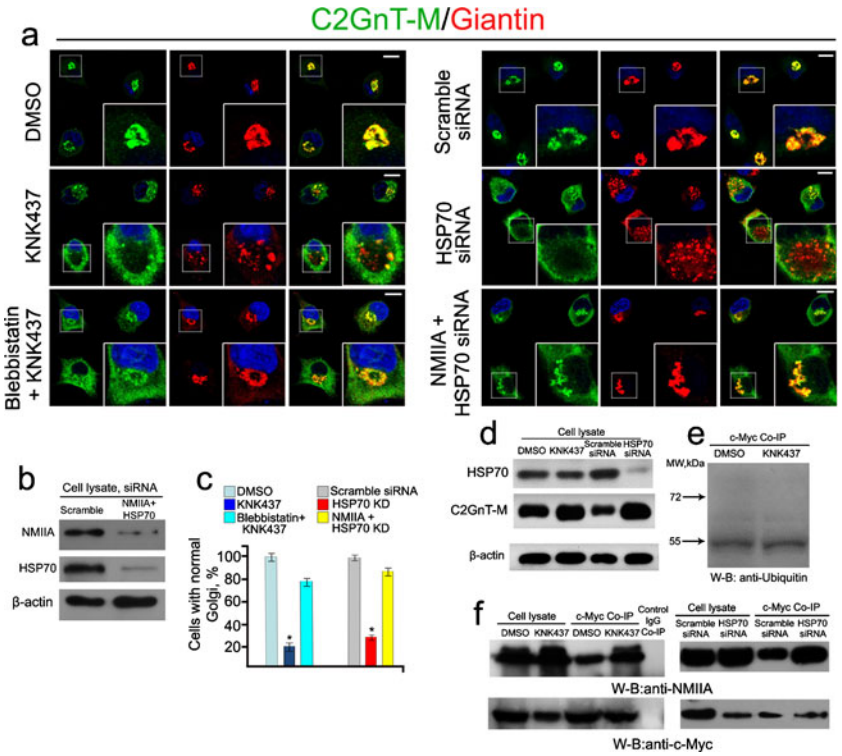

Fig. 5 NMIIA is involved in Golgi fragmentation induced by inhibition or knockdown of HSP70 in Panc1-bC2GnT-M (c-Myc) cells. **a** Confocal immunofluorescence images of bC2GnT-M and giantin. Inhibition of HSPs (with 100 μM KNK437) or KD of HSP70 (250 nM of HSP70-8 siRNA) caused Golgi fragmentation, which was accompanied by increased bC2GnT-M fluorescence intensity. These effects were blocked by pretreatment with blebbistatin or NMIIA siRNA. *White boxes* of the images indicate representative cells enlarged in the inset. **b** NMIIA and HSP70 western blot of the lysates of cells treated with scramble or NMIIA (*MYH9*)+HSP70 (*HSPA8*) siRNAs; beta-actin was used as a loading control. **c** Percentage of the cells with unaffected Golgi in cells treated with DMSO, KNK437, and blebbistatin followed by KNK437 or scramble siRNA, HSP70 siRNA, or NMIIA+HSP70 siRNAs. The data are expressed as mean±SEM; *Asterisk*, $p<0.001$ for KNK437 vs. DMSO or blebbistatin+KNK437 and HSP70 siRNA vs. scramble siRNA or NMIIA+HSP70 siRNAs. **d** Inhibition of HSPs or KD of HSP70 increased C2GnT-M as assessed by western blotting. **e** Ubiquitin western blot of complexes pulled down with anti-c-Myc Abs from the lysates of cells treated with DMSO or KNK437. **f** NMIIA and c-Myc western blot of the complexes pulled down with anti-c-Myc Ab from the lysates of cells treated with DMSO, KNK437, scramble siRNA, or HSP70 siRNA. Lysates containing the same amounts of NMIIA were used for c-Myc Co-IP. The results shown are representative of three independent experiments. All confocal images were acquired with same imaging parameters; bars, 10 μm.

an apparent effect on the Golgi morphology as shown by immunostaining of a Golgi matrix protein giantin (Fig. 6d). Extensive fragmentation of the Golgi was observed after treatment with 10 μM of GA for 2 h. However, treatment of the cells with blebbistatin followed by 10 μM GA retained C2GnT-M in the Golgi and preserved the compact Golgi morphology (Fig. 6d, g). Similarly, cells treated with 200 nM HSP90β1 siRNA, which resulted in 95 % KD HSP90β1 (Fig. 6f), yielded fragmented Golgi, while the Golgi morphology in cells treated by HSP90β1 plus NMIIA siRNAs was similar to that of the control (Fig. 6e–g). In addition, we observed a drastic decrease of C2GnT-M after treatment with 10 μM GA for 2 h (Fig. 6h) and a huge increase of polyubiquitinated C2GnT-M after treatment for 1 h (Fig. 6i). Next, we found that treatment of cells with either 10 μM of GA or 200 nM HSP90β1 siRNA increased the C2GnT-M–NMIIA complexes (Fig. 6i). To examine the role of C2GnT-M in GA-induced Golgi fragmentation, we monitored the C2GnT-M dose effect on Golgi fragmentation in cells treated with 10 μM GA for 2 h by taking advantage of the Panc1-bC2GnT-M (c-Myc) cells which expressed heterogeneous levels of bC2GnT-M (Petrosyan and Cheng 2013) and by analyzing the relationship of bC2GnT-M fluorescence intensity with number of cells with fragmented Golgi. As shown in Fig. 6j, in cells with a high level of bC2GnT-M (top and left), the giantin staining was fragmented; however, in cells expressing little, if any, amount of bC2GnT-M (right and bottom), the Golgi appeared like a single compact structure. The calculated Spearman's rank correlation coefficient between number of Golgi fragments and C2GnT-M fluorescence was 0.69 ($p<0.01$) (Fig. 6k). These data not only confirm the importance of C2GnT-M as a binding protein

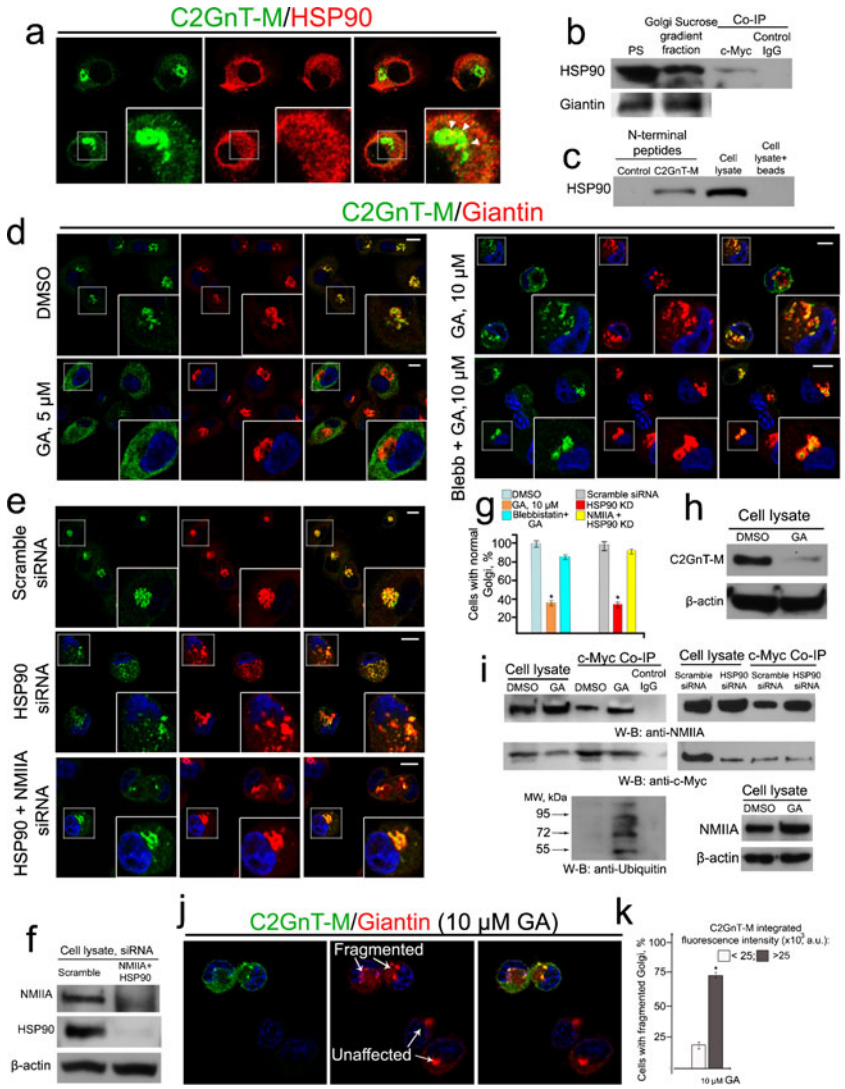

Fig. 6 NMIIA is required for Golgi breakdown induced by inhibition or knockdown of HSP90 in Panc1-bC2GnT-M (c-Myc) cells. **a** Confocal immunofluorescence images of C2GnT-M and HSP90: co-staining was detected at the periphery of the Golgi (*white arrowheads*). **b** C2GnT-M and HSP90 were associated in the Golgi. Golgi membranes were isolated from control cells as described in "Materials and methods" and 25 μg of total protein of Golgi or postnuclear supernatant was immunoblotted to detect giantin and HSP90. Note that HSP90 is abundantly present in Golgi membranes. The Golgi fraction was subjected to Co-IP with c-Myc Ab. **c** HSP90 western blot of the complexes pulled down from cell lysates with biotinylated control peptide or hC2GnT-M N-terminal peptide, cell lysate, and cell lysate proteins isolated by magnetic beads without peptides. **d** Confocal immunofluorescence images of bC2GnT-M and giantin in cells treated with 5 or 10 μM geldanamycin (GA), or 35 μM blebbistatin (Blebb) followed by 10 μM GA. **e** Confocal immunofluorescence images of bC2GnT-M and giantin in cells treated with scramble, HSP90 beta isoform (*HSP 90*β) siRNA, or NMIIA+HSP90 siRNAs. *White boxes* of the images indicate representative cells enlarged in the inset. **f** NMIIA and HSP90 western blots of the lysates of cells treated with scramble siRNA or NMIIA (*MYH9*)+HSP90 (*HSP 90*β) siRNAs; β-actin was used as a loading control. **g** Percentage of the cells with unaffected Golgi in cells described in **d** and **e**: KD/inhibition of NMIIA retards Golgi fragmentation induced by KD/inhibition of HSP90, respectively; *Asterisk*, $p<0.001$. **h** c-Myc western blot of the lysates of cells treated with 10 μM GA or appropriate amount of DMSO for 2 h. **i** NMIIA, c-Myc, and ubiquitin western blot of complexes pulled down with anti-c-Myc Ab from the lysates of cells treated with 10 μM GA/appropriate amount of DMSO for 1 h or scramble siRNA/HSP90 siRNA for 48 h. Cell lysates containing the same amounts of NMIIA were used for c-Myc Co-IP. NMIIA western blot of the lysates of cells treated with 10 μM GA or appropriate amount of DMSO for 1 h. **j** Confocal immunofluorescence images of bC2GnT-M and giantin in Panc1-bC2GnT-M (c-Myc) cells treated with 10 μM of GA for 1 h. The fragmentation of Golgi was analyzed in 90 cells with low (up to 25,000 a.u.) or high (over 25,000 a.u.) C2GnT-M integrated fluorescence. Note that the response to GA treatment (*white arrows*) in cells with high C2GnT-M was more pronounced than in ones with low C2GnT-M. **k** Percentage of the cells with fragmented Golgi in cells described in **j**.

for NMIIA but also show that in Panc1-bC2GnT-M cells, the efficiency of GA-induced fragmentation of the Golgi directly depends on intra-Golgi concentration of C2GnT-M and, consequently, the extent of C2GnT-M and NMIIA interaction.

Discussion

Morphological changes of Golgi apparatus occur under certain normal physiological conditions and stress (White et al. 2001; Hicks and Machamer 2005). However, the mechanisms are not completely understood. Previously, NMIIA was found to be closely associated with Golgi membrane and involved in intracellular vesicular trafficking (Stow et al. 1998) and brefeldin A-induced Golgi collapse (Durán et al. 2003; Petrosyan et al. 2012a). Recently, we observed that NMIIA interacts with Golgi GT, which participates in Golgi remodeling under basal conditions and Golgi disorganization induced by treatment with brefeldin A or KD of β-COP (Petrosyan et al. 2012b; Petrosyan and Cheng 2013). Further, this interaction leads to degradation of these enzymes by proteasome. The current study extends this observation by showing that the Golgi fragmentation induced by HS treatment or inhibition/depletion of HSP is also mediated by NMIIA via its interaction with Golgi GTs. However, proteasome degradation of GTs occurs only under HS treatment or inhibition/depletion of HSP90 but not in the inhibition or KD of HSP70. Further, recovery of Golgi morphology following HS treatment precedes the return of GTs to the Golgi.

It has been well established that HS induces numerous cellular stress responses, which include upregulation of HSP (Welch 1992), elevated protein degradation following ubiquitination (Medicherla and Goldberg 2008; Carlson et al. 1987), and Golgi disorganization (Wang et al. 1998). It was not clear how these seemingly diverse phenomena induced by HS are linked. The current study provides evidences which explain how these phenomena occur.

We have found that the HS-induced Golgi fragmentation is mediated by NMIIA via its interaction with Golgi GTs. Further, HS-induced Golgi disorganization is positively correlated with the levels of Golgi GTs regardless of whether these enzymes are ectopically or endogenously expressed. These results confirm our recent reports of the involvement of NMIIA in the Golgi remodeling under normal cellular processes and Golgi fragmentation under stress through its interaction with Golgi GTs (Petrosyan et al. 2012a; Petrosyan and Cheng 2013). We have also observed that HSP70 is elevated about 8 h after 20 min of HS treatment, which persists thereafter. It is important to note that HS induces a quick distribution of GT to the cytoplasm, which conceivably leads to overburden of the cellular proteolytic system. Indeed, we have detected ubiquitination of the Golgi enzymes within only 20 min of HS treatment. In light of this, the increase of HSP70 as a part of stress response, especially as a consequence of HS, might be considered as the compensatory mechanism because HSP70 is also involved in proteasome-mediated protein degradation (McDonough and Patterson 2003; Robertson et al. 1999; Ryhänen et al. 2009). As a result, at 12 h post HS, the NMIIA–C2GnT-M complexes are elevated (Fig. 3c) and the amount of C2GnT-M is decreased (Fig. 3b). It is noteworthy that the NMIIA–C2GnT-M complexes return to the basal level at 18 h and remain unchanged at 24 and 36 h post HS (Fig. 3c). On the contrary, the amount of C2GnT-M after temporal normalization was increased at these two time points (Fig. 3b). Meantime, the induction of HSP70 is a cellular response to HS-induced production of misfolded proteins, such as Golgi GTs (Goldberg 2003). We assume that a large fraction of newly synthesized GT is degraded because of unsuccessful folding but may aggregate prior to degradation (Sherman and Goldberg 2001; Schubert et al. 2000). On the other hand, the retention of these enzymes in the ER might be resulted from a decrease of their proteolysis (Carlson et al. 1987; Kuckelkorn et al. 2000). Altogether, it can explain the phenomenon of increased C2GnT-M at 24 and 36 h post HS.

It is of interest to note that the HS response is transient, and here we show for the first time that post-HS Golgi reassembly is a staged process. Although the normal morphology of Golgi, which consisted of matrix and resident proteins, is recovered after 36 h post HS, there is a difference in the kinetics of recovery between Golgi matrix proteins and GTs. It takes about 18–24 h for the matrix proteins to regenerate the Golgi morphology, but about 36 h post HS for GTs to come back to the Golgi. Therefore, after HS, the restoration of the Golgi morphology precedes the return of GTs to the Golgi. This phenomenon is in agreement with the concept that matrix proteins are the backbone of the Golgi morphology, and targeting of Golgi GTs requires the presence of these golgins in the Golgi (Petrosyan et al. 2012b).

The treatment of Panc1-bC2GnT-M (c-Myc) cells with high concentrations of HSP inhibitor KNK437 (100 μM) or HSP70 siRNA (250 nM) results in the retention of C2GnT-M in the cytosol and disorganization of the Golgi. The rescue of the Golgi morphology that contains C2GnT-M after treatment with blebbistatin indicates that the interaction of NMIIA with this enzyme is responsible for the Golgi fragmentation induced by HSP70 inhibition or KD. Further, inhibition/depletion of HSP70 increases the levels of NMIIA–bC2GnT-M complexes. Therefore, the driving force for the induction of Golgi fragmentation is the same for HS and HSP inhibition/KD. It should be mentioned that the high levels of C2GnT-M present in the cytosol of the cells treated with blebbistatin+KNK437 or NMIIA+HSP70 siRNAs likely represent unfolded C2GnT-M that fails to leave the ER because C2GnT-M cannot be folded properly without HSP70. However, there is one major difference in the downstream effect between HS and HSP70 inhibition/depletion. HS enhances ubiquitination and proteasomal degradation of C2GnT-M while inhibition/depletion of HSP70 does not. The result is in agreement with the essential role HSP70 plays in proteasomal degradation of proteins. In addition, like HSP inhibitor KNK437 or KD of HSP70, HSP90 inhibitor GA also exhibits differential concentration effect on Golgi morphology

and distribution of Golgi residential proteins. At low concentration (5 μM), GA retains C2GnT-M in the ER without affecting the Golgi morphology. At high concentration (10 μM), GA induces Golgi fragmentation. This effect is reproduced in cells treated with HSP90 siRNA. However, there is a difference in the effect of KNK437 (100 μM) versus that of GA (10 μM). Although both treatments increase the formation of NMIIA–bC2GnT-M complexes, GA treatment enhances ubiquitination and degradation of bC2GnT-M while KNK437 treatment does not. The difference in this effect is likely the result of the different functions of these two HSP: HSP90 is involved in the folding of newly synthesized proteins and not proteasomal degradation of ubiquitinated proteins, while HSP70 is involved in both processes. Therefore, inhibition or depletion of HSP90 would compromise the protein folding but not the function of proteasome, which results in degradation of the proteins (Whitesell et al. 1997; Mimnaugh et al. 2004), an effect different from that of inhibition/depletion of HSP70 as described above.

On the basis of current knowledge, HSPs are also involved in many intra-Golgi processes. For example, HSP70 controls SNARE complex formation, and both HSP70 and HSP90 have been found in trafficking and targeting of lipopolysaccharides to the Golgi apparatus (Triantafilou and Triantafilou 2004; Joglekar and Hay 2005). Further, Hsp90 chaperone system may function as a general regulator of Rab GTPase recycling and is thereby essential for Rab1-dependent Golgi assembly (Chen and Balch 2006). These observations fit well with our data, suggesting that HSP90 may function not only as a classical ER chaperone but also a stabilizer for GTs in the Golgi through interaction with their cytoplasmic tails. However, details of such interaction and sequence of events (GT-HSP90 and GT-NMIIA) need further investigations.

In summary, we have provided the mechanism of Golgi fragmentation induced by either HS or inhibition/depletion of HSP. We have shown that this phenomenon requires the interaction of NMIIA with Golgi GTs. Under basal conditions, this interaction is responsible for Golgi remodeling mediated by NMIIA-dependent transport of Golgi residential proteins to the ER for recycling. Under stress, such as HS or inhibition of HSP, formation of NMIIA–GT complexes is required for Golgi fragmentation. However, many questions remain. For example, how are the NMIIA–GT complexes upregulated and how is the Golgi instability induced by heat shock and inhibition of HSPs? We suppose that the generation of the tension by NMIIA and C2GnT-M is a more complicated mechanism and requires the participation of other players also. Given the rapid response of Golgi fragmentation to HS, alteration of the functions of some bona fide Golgi-associated proteins through phosphorylation/dephosphorylation is one likely cause. The GTPase Rab1 in the Golgi membranes (Tomás et al. 2012) and B cell lymphoma 2-associated athanogene protein-1, which is a negative regulator of HSP70 and a protein involved in the maintenance of Golgi morphology by targeting to the COPI-coated structures, represent some of these proteins (Bimston et al. 1998; Takamura et al. 2003). In the case of Golgi fragmentation induced by inhibition/deletion of HSP, failure of ER-to-Golgi trafficking of critical proteins responsible for maintaining the morphology of the Golgi may be a contributor because loss of HSP70 or 90 can lead to their misfolding. The key then is to identify the proteins that help maintain the integrity of the Golgi morphology of which functions are compromised under HS or inhibition/depletion of HSP70/90.

Acknowledgments We thank Mrs. Helen Cheng for her excellent technical assistance and Ms. Janice A. Taylor at the Confocal Microscopy Core Facility for her assistance in confocal immunofluorescence microscopy. This work is supported in part by the Office of Research and Development, Medical Research Service, Department of Veterans Affairs (VA 1I1BX000985) and the State of Nebraska (LB506).

References

Allan VJ, Thompson HM, McNiven MA (2002) Motoring around the Golgi. Nat Cell Biol 4:236–242

Ali MF, Chachadi VB, Petrosyan A, Cheng PW (2012) Golgi phosphoprotein 3 determines cell binding properties under dynamic flow by controlling Golgi localization of core 2 *N*-acetylglucosaminyltransferase 1. J Biol Chem 287:39564–39577

Barr FA, Short B (2003) Golgins in the structure and dynamics of the Golgi apparatus. Curr Opin Cell Biol 15:405–413

Bimston D, Song J, Winchester D, Takayama S, Reed JC, Morimoto RI (1998) BAG-1, a negative regulator of Hsp70 chaperone activity, uncouples nucleotide hydrolysis from substrate release. EMBO J 17:6871–6878

Burke J, Pettitt JM, Humphris D, Gleeson PA (1994) Medial-Golgi retention of *N*-acetylglucosaminyltransferase I. Contribution from all domains of the enzyme. J Biol Chem 269:12049–12059

Carlson N, Rogers S, Rechsteiner M (1987) Microinjection of ubiquitin: changes in protein degradation in HeLa cells subjected to heat-shock. J Cell Biol 104:547–555

Chen CY, Balch WE (2006) The Hsp90 chaperone complex regulates GDI-dependent Rab recycling. Mol Biol Cell 17:3494–3507

Choi KH, Basma H, Singh J, Cheng PW (2005) Activation of CMV promoter-controlled glycosyltransferase and beta-galactosidase glycogenes by butyrate, tricostatin A, and 5-aza-2′-deoxycytidine. Glycoconj J 22:63–69

Durán JM, Valderrama F, Castel S, Magdalena J, Tomás M, Hosoya H, Renau-Piqueras J, Malhotra V, Egea G (2003) Myosin motors and not actin comets are mediators of the actin-based Golgi-to-endoplasmic reticulum protein transport. Mol Biol Cell 14:445–459

Egea G, Francí C, Gambús G, Lesuffleur T, Zweibaum A, Real FX (1993) cis-Golgi resident proteins and O-glycans are abnormally compartmentalized in the RER of colon cancer cells. J Cell Sci 105:819–830

Fath KR (2005) Characterization of myosin-II binding to Golgi stacks in vitro. Cell Motil Cytoskeleton 60:222–235

Gao Y, Chachadi VB, Cheng PW, Brockhausen I (2012) Glycosylation potential of human prostate cancer cell lines. Glycoconj J 29:525–537

Grabenhorst E, Conradt HS (1999) The cytoplasmic, transmembrane, and stem regions of glycosyltransferases specify their in vivo functional sublocalization and stability in the Golgi. J Biol Chem 274:36107–36116

Graves TK, Patel S, Dannies PS, Hinkle PM (2001) Misfolded growth hormone causes fragmentation of the Golgi apparatus and disrupts endoplasmic reticulum-to-Golgi traffic. J Cell Sci 114:3685–3694

Grad I, Picard D (2007) The glucocorticoid responses are shaped by molecular chaperones. Mol Cell Endocrinol 275:2–12

Goldberg AL (2003) Protein degradation and protection against misfolded or damaged proteins. Nature 426:895–899

Gonatas NK, Stieber A, Gonatas JO (2006) Fragmentation of the Golgi apparatus in neurodegenerative diseases and cell death. J Neurol Sci 246:21–30

Hicks SW, Machamer CE (2005) Golgi structure in stress sensing and apoptosis. Biochim Biophys Acta 1744:406–414

Hu W, Xu R, Zhang G, Jin J, Szulc ZM, Bielawski J, Hannun YA, Obeid LM, Mao C (2005) Golgi fragmentation is associated with ceramide-induced cellular effects. Mol Biol Cell 16:1555–1567

Joglekar AP, Hay JC (2005) Evidence for regulation of ER/Golgi SNARE complex formation by hsc70 chaperones. Eur J Cell Biol 8:529–542

Kellokumpu S, Sormunen R, Kellokumpu I (2002) Abnormal glycosylation and altered Golgi structure in colorectal cancer: dependence on intra-Golgi pH. FEBS Lett 516:217–224

Klausner RD, Donaldson JG, Lippincott-Schwartz J (1992) Brefeldin A: insights into the control of membrane traffic and organelle structure. J Cell Biol 116:1071–1080

Kuckelkorn U, Knuehl C, Boes-Fabian B, Drung I, Kloetzel PM (2000) The effect of heat shock on 20S/26S proteasomes. Biol Chem 381:1017–1023

Kumemura H, Harada M, Omary MB, Sakisaka S, Suganuma T, Namba M, Sata M (2004) Aggregation and loss of cytokeratin filament networks inhibit golgi organization in liver-derived epithelial cell lines. Cell Motil Cytoskeleton 57:37–52

Marsh BJ (2002) Howell KE (2002) The mammalian Golgi–complex debates. Nat Rev Mol Cell Biol 3:789–795

Medicherla B, Goldberg AL (2008) Heat shock and oxygen radicals stimulate ubiquitin-dependent degradation mainly of newly synthesized proteins. J Cell Biol 182:663–673

McDonough H, Patterson C (2003) CHIP: a link between the chaperone and proteasome systems. Cell Stress Chaperones 8:303–308

Mimnaugh EG, Xu W, Vos M, Yuan X, Isaacs JS, Bisht KS, Gius D, Neckers L (2004) Simultaneous inhibition of hsp 90 and the proteasome promotes protein ubiquitination, causes endoplasmic reticulum-derived cytosolic vacuolization, and enhances antitumor activity. Mol Cancer Ther 3:551–566

Morré DJ, Mollenhauer HH (2009) The Golgi apparatus: the first 100 years. Springer Science + Business Media, New York

Numata Y, Morimura T, Nakamura S, Hirano E, Kure S, Goto YI, Inoue K (2013) Depletion of molecular chaperones from the endoplasmic reticulum and fragmentation of the Golgi apparatus associated with pathogenesis in Pelizaeus–Merzbacher disease. J Biol Chem 288:7451–7466

Osman N, McKenzie IF, Mouhtouris E, Sandrin MS (1996) Switching amino-terminal cytoplasmic domains of alpha(1,2)fucosyltransferase and alpha(1,3)galactosyltransferase alters the expression of H substance and Galalpha(1,3)Gal. J Biol Chem 271:33105–33109

Paulson JC, Colley KJ (1989) Glycosyltransferases. Structure, localization, and control of cell type-specific glycosylation. J Biol Chem 264:17615–17618

Pavelka M, Ellinger A (1983) Effect of colchicine on the Golgi complex of rat pancreatic acinar cells. J Cell Biol 97:737–748

Petrosyan A, Ali MF, Verma SK, Cheng H, Cheng PW (2012a) Non-muscle myosin IIA transports a Golgi glycosyltransferase to the endoplasmic reticulum by binding to its cytoplasmic tail. Int J Biochem Cell Biol 44:1153–1165

Petrosyan A, Ali MF, Cheng PW (2012b) Glycosyltransferase-specific Golgi targeting mechanisms. J Biol Chem 287:37621–37627

Petrosyan A, Cheng PW (2013) A non-enzymatic function of Golgi glycosyltransferases: mediation of Golgi fragmentation by interaction with non-muscle myosin IIA. Glycobiology 23:690–708

Pfeffer SR (2001) Constructing a Golgi complex. J Cell Biol 155:873–875

Puri S, Telfer H, Velliste M, Murphy RF, Linstedt AD (2004) Dispersal of Golgi matrix proteins during mitotic Golgi disassembly. J Cell Sci 117:451–466

Robertson JD, Datta K, Biswal SS, Kehrer JP (1999) Heat-shock protein 70 antisense oligomers enhance proteasome inhibitor-induced apoptosis. Biochem J 344:477–485

Rogalski AA, Bergmann JE, Singer SJ (1984) Effect of microtubule assembly status on the intracellular processing and surface expression of an integral protein of the plasma membrane. J Cell Biol 99:1101–1109

Rosso S, Bollati F, Bisbal M, Peretti D, Sumi T, Nakamura T, Quiroga S, Ferreira A, Cáceres A (2004) LIMK1 regulates Golgi dynamics, traffic of Golgi-derived vesicles, and process extension in primary cultured neurons. Mol Biol Cell 15:3433–3449

Ryhänen T, Hyttinen JM, Kopitz J, Rilla K, Kuusisto E, Mannermaa E, Viiri J, Holmberg CI, Immonen I, Meri S, Parkkinen J, Eskelinen EL, Uusitalo H, Salminen A, Kaarniranta K (2009) Crosstalk between Hsp70 molecular chaperone, lysosomes and proteasomes in autophagy-mediated proteolysis in human retinal pigment epithelial cells. J Cell Mol Med 13:3616–3631

Sahlender DA, Roberts RC, Arden SD, Spudich G, Taylor MJ, Luzio JP, Kendrick-Jones J, Buss F (2005) Optineurin links myosin VI to the Golgi complex and is involved in Golgi organization and exocytosis. J Cell Biol 169:285–295

Siddhanta A, Radulescu A, Stankewich MC, Morrow JS, Shields D (2003) Fragmentation of the Golgi apparatus. A role for beta III spectrin and synthesis of phosphatidylinositol 4,5-bisphosphate. J Biol Chem 278:1957–1965

Sherman MY, Goldberg AL (2001) Cellular defenses against unfolded proteins: a cell biologist thinks about neurodegenerative diseases. Neuron 29:15–32

Stebbins CE, Russo AA, Schneider C, Rosen N, Hartl FU, Pavletich NP (1997) Crystal structure of an Hsp90-geldanamycin complex: targeting of a protein chaperone by an antitumor agent. Cell 89:239–250

Schubert U, Antón LC, Gibbs J, Norbury CC, Yewdell JW, Bennink JR (2000) Rapid degradation of a large fraction of newly synthesized proteins by proteasomes. Nat Geosci 404:770–774

Stow JL, Fath KR, Burgess DR (1998) Budding roles for myosin II on the Golgi. Trends Cell Biol 8:138–141

Straight AF, Cheung A, Limouze J, Chen I, Westwood NJ, Sellers JR, Mitchison TJ (2003) Dissecting temporal and spatial control of cytokinesis with a myosin II inhibitor. Science 299:1743–1747

Takamura A, Adachi M, Wada I, Mitaka T, Takayama S, Imai K (2003) Accumulation of Hsp70/Hsc70 molecular chaperone regulator BAG-1 on COPI-coated structures in gastric epithelial cells. Int J Oncol 23:1301–1308

Tomás M, Marín MP, Martínez-Alonso E, Esteban-Pretel G, Díaz-Ruiz A, Vázquez-Martínez R, Malagón MM, Renau-Piqueras J, Martínez-Menárguez JA (2012) Alcohol induces Golgi fragmentation in differentiated PC12 cells by deregulating Rab1-dependent ER-to-Golgi transport. Histochem Cell Biol 138:489–501

Triantafilou M, Triantafilou K (2004) Heat-shock protein 70 and heat-shock protein 90 associate with Toll-like receptor 4 in response to bacterial lipopolysaccharide. Biochem Soc Trans 32:636–639

Uliana AS, Giraudo CG, Maccioni HJ (2006) Cytoplasmic tails of SialT2 and GalNAcT impose their respective proximal and distal Golgi localization. Traffic 7:604–612

Wang TT, Chiang AS, Chu JJ, Cheng TJ, Chen TM, Lai YK (1998) Concomitant alterations in distribution of 70 kDa heat shock

proteins, cytoskeleton and organelles in heat shocked 9L cells. Int J Biochem Cell Biol 30:745–759

Ward TH, Polishchuk RS, Caplan S, Hirschberg K, Lippincott-Schwartz J (2001) Maintenance of Golgi structure and function depends on the integrity of ER export. J Cell Biol 155:557–570

Welch WJ, Suhan JP (1985) Morphological study of the mammalian stress response: characterization of changes in cytoplasmic organelles, cytoskeleton, and nucleoli, and appearance of intranuclear actin filaments in rat fibroblasts after heat-shock treatment. J Cell Biol 101:1198–211

Welch WJ (1992) Mammalian stress response: cell physiology, structure/function of stress proteins, and implications for medicine and disease. Physiol Rev 72:1063–1081

White J, Keller P, Stelzer EH (2001) Spatial partitioning of secretory cargo from Golgi resident proteins in live cells. BMC Cell Biol 2:19

Whitesell L, Sutphin P, An WG, Schulte T, Blagosklonny MV, Neckers L (1997) Geldanamycin-stimulated destabilization of mutated p53 is mediated by the proteasome in vivo. Oncogene 14:2809–2816

Xu YX, Liu L, Caffaro CE, Hirschberg CB (2010) Inhibition of Golgi apparatus glycosylation causes endoplasmic reticulum stress and decreased protein synthesis. J Biol Chem 285:24600–24608

Yokota S, Kitahara M, Nagata K (2000) Benzylidene lactam compound, KNK437, a novel inhibitor of acquisition of thermotolerance and heat shock protein induction in human colon carcinoma cells. Cancer Res 60:2942–2948